Vol 13 No 2, February 2004
1009-1963/2004/13(02)/0251-07

Chinese Physics

© 2004 Chin. Phys. Soc.
and IOP Publishing Ltd

Critical properties of XY model on two-layer Villain–ferromagnetic lattice *

Wang Yi(王 漪)[a)b)†], R. Quartu [b)], Liu Xiao-Yan(刘晓彦)[a)],
Han Ru-Qi(韩汝琦)[a)], and Horiguchi Tsuyoshi(堀口刚)[b)]

[a)] *Institute of Microelectronics, Peking University, Beijing* 100871, *China*

[b)] *Department of Computer and Mathematical Sciences, GSIS, Tohoku University* 04, *Sendai* 980-8579, *Japan*

(Received 16 May 2003; revised manuscript received 14 July 2003)

We investigate phase transitions of the XY model on a two-layer square lattice which consists of a Villain plane (J) and a ferromagnetic plane (I), using Monte Carlo simulations and a histogram method. Depending on the values of interaction parameters (I, J), the system presents three phases: namely, a Kosterlitz–Thouless (KT) phase in which the two planes are critical for I predominant over J, a chiral phase in which the two planes have a chiral order for J predominant over I and a new phase in which only the Villain plane has a chiral order and the ferromagnetic plane is paramagnetic with a small value of chirality. We clarify the nature of phase transitions by using a finite size scaling method. We find three different kinds of transitions according to the values of (I, J): the KT transition, the Ising transition and an XY-Ising transition with $\nu = 0.849(3)$. It turns out that the Ising or XY-Ising transition is associated with the disappearance of the chiral order in the Villain plane.

Keywords: XY model, chirality, KT transition, two-layer Villain lattice
PACC: 7510H, 7540C, 0570F, 0550

1. Introduction

Due to the development of the epitaxy technology, it has been possible to study magnetic properties of very thin magnetic films. It is shown that the thin films present several phases such as the antiferromagnetic phase with surface spins parallel to the external magnetic field H, the antiferromagnetic phase with surface spins anti-parallel to H, the surface spin flop phase and the bulk spin flop phase, and so on.[1−4] However, theoretical investigations of the magnetic thin films have been done mainly for the ground-state properties by phenomenological treatment or for the finite temperature properties by mean field approximation.[5−7] There has been little investigation from the standpoint of statistical physics for the frustrated spin system.[8]

On the other hand, the critical behaviour of two-dimensional (2D) fully frustrated (FF) XY models has been investigated extensively over many years.[9−16] The reason for this interest is that the nature of the phase transition is not yet understood. In those models, there coexists Z_2 chiral symmetry of the Ising-spin type in addition to the continuous $U(1)$ symmetry associated with the global rotation of XY spins. The breaking of the chiral symmetry Z_2 gives rise to an Ising transition while that of the rotation of the XY spins to the Kosterlitz–Thouless (KT) transition. There are several contradictory suggestions for these transitions. Some authors have claimed that the Ising transition and the KT transition occur at the same temperature in a coupled or decoupled manner. Other authors have claimed that the transitions occur at different temperatures. In the latter case, the two transitions can be the KT transition and an Ising transition, respectively, or the KT transition and a new kind of transition, respectively.

Berge *et al*[9] investigated the nature of phase transition in a generalized uniformly frustrated XY model on the square lattice. Changing the negative bond strength varies the strength of frustration. They suggested the existence of an Ising transition and the KT transition. But, in the fully frustrated case, these

*Project supported by the Scientific Research Foundation for the Returned Overseas Chinese Scholars, State Education Ministry, and the National Natural Science Foundation of China (Grant No 10234010).

†Tel: (010) 62756745; E-mail: wangyi@ime.pku.edu.cn

two transitions are merged into a single one of dominant Ising character. This scenario of a single transition has been supported by a number of studies that give the following value for the critical exponent: $\nu = 0.85(3)$ [10,11] or $\nu = 0.852(2)$.[12] This suggests a new universality class, the so-called XY Ising class for the transition occurring in this model. There is a possibility that a new universality class arises also in the case of a frustrated Heisenberg or XY model on the stacked triangular lattice. However, other authors suggested the existence of two distinct phase transitions. Lee and Lee [13] investigated the FF XY model on the square lattice using a microcanonical Monte Carlo (MC) technique. They found that the system has two separate phase transitions. At the lower critical temperature, they found the KT transition. At the higher critical temperature, they found a transition related to the melting of the vortex lattice with critical exponent $\nu = 0.813(5)$. In the same model, by using the real-space renormalization group approach, Jeon *et al* [14] showed that the KT and the Ising types of transition occur at different temperatures. Ramirez-Santiago and Jose [15] found also two phase transitions. The chiral transition occurs at the lower critical temperature with $\nu = 0.875(35)$, which is different from the expected value for the 2D Ising critical exponent. The KT transition occurs at the higher critical temperature with a value of exponent different from that of the usual unfrustrated XY model. Olsson has also found two distinct transitions in the same model.[16] He found $\nu = 1$ as in the standard 2D Ising model, in contradiction with results from papers cited above.

As an example of very thin magnet films, an XY model on a two layer triangular lattice has recently been investigated from a standpoint of statistical physics.[8] In that study, it was shown that there exist three kinds of transitions in the system: namely, the usual KT transition, the Ising transition and a new chiral transition. This chiral transition occurs between two different chiral phases: a phase with a 120°-structure in a triangular lattice and a phase with an angle between the spins depending of the interaction values in the other triangular lattice. The values of critical exponents were given as $\nu = 0.92(8)$, $\alpha = 0.29(9)$ and $\beta = 0.253(3)$.

We investigate the nature of phase transitions for the XY model on a lattice on a two-layer square planes in the present paper. We consider the XY model with a ferromagnetic intralayer on one of two layers and a Villain plane. Namely, by using standard MC simulations and the so-called MC histogram technique, we investigate the XY model on a two-layer square lattice. We find three kinds of transitions, namely, the standard 2D Ising transition, the KT transition and the XY Ising transition. The result shows that the phase transition of the XY model on a two-layer square lattice is different from the XY model on a two-layer triangular lattice.[8]

We describe our model and give a phase diagram of the ground state in Section 2. In Section 3, we give the results obtained by means of extensive histogram MC simulations and discuss the nature of phase transitions in terms of finite-size scaling analysis. A phase diagram in an interaction parameter versus temperature plane is obtained. Concluding remarks are given in Section 4.

2. XY model on two-layer Villain–ferromagnetic lattice

We consider a system descried by the following Hamiltonian: Λ_1, $\Lambda_2, N = |\Lambda_1| = |\Lambda_2| = N_{\rm l} \times N_{\rm l}$:

$$\mathcal{H} = -\sum_{(ij)} J_{ij} \boldsymbol{s}_i \cdot \boldsymbol{s}_j - I \sum_{(ij)} \boldsymbol{t}_i \cdot \boldsymbol{t}_j - K \sum_i \boldsymbol{s}_i \cdot \boldsymbol{t}_i, \quad (1)$$

where s_i and t_i are XY spins on the Villain plane (VP) and on the ferromagnetic plane (FP), respectively. In the VP, the nearest-neighbour interaction constant J_{ij} is equal to J for the bond represented by a thin line and to J' for the bond represented by a thick line in Fig.1. In the present paper, we consider only the fully frustrated case in which $J = -J'$. In the FP, the nearest-neighbour interaction constant is equal to I and hence there is no frustration. The interplane interaction constant between the VP and the FP is denoted by K. We note that there is a relation $Q(J, I, K) = Q(J, I, -K)$ for a thermodynamic quantity $Q(J, I, K)$ and, hence, we assume $K > 0$ without loss of generality. The sum with (ij) indicates a summation over the nearest-neighbour pairs of sites on the VP or the FP. The sum with i indicates a summation over the pairs of sites i on the VP and the FP.

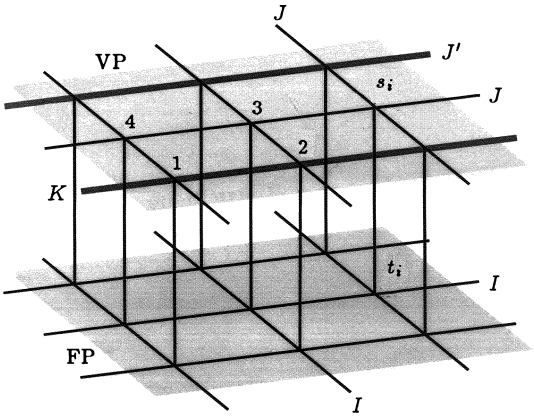


Fig.1. Two-layer Villain–ferromagnetic lattice, VP and FP. The XY spins are denoted s_i on VP and t_i on FP. The intralayer interaction constants are J with pattern of ferromagnetic (thin) and J' antiferromagnetic (thick) bonds on VP, I on FP and the interlayer infraction constant is K.

Now, we recall the ground-state configuration of the VP.[9] The spin configuration depends on the values of J and J'. When $\eta = -J'/J$, the system is in the ferromagnetic or antiferromagnetic phase. When $\eta > 1/3$ the spins are canted. The angles between the spins on a nearest-neighbour pair of sites are equal to Q for the spins linked by a ferromagnetic bond and $3Q$ for the spins linked by an antiferromagnetic bond. Here Q is given by the relation $\cos Q = \frac{1}{2}\sqrt{\frac{\eta+1}{\eta}}$. Hence in the fully frustrated case, where $\eta = 1$, the spin configuration is given by $Q = 45°$ and $3Q = 135°$. For $J > 0$ the angles between the spins linked by the ferromagnetic bonds J are equal to 45°. We call this configuration the 45° configuration. For $J < 0$, the angles between the spins linked by the antiferromagnetic bonds J are equal to 135°. We call this configuration the 135° configuration.

We have used a numerical method for minimizing the energy in order to find the ground-state configurations. The shape of the phase diagram is qualitatively the same for different values of K. In Fig.2, we have plotted the ground-state phase diagram in the space of I versus J' for $K = 0.5$. According to the values of interaction parameters (I, J'), the system presents three phases in the ground state:

(i) A ferromagnetic phase (Ferro), in which the two phases are ferromagnetically ordered, when I is positive and predominant in comparison with J'.

(ii) An antiferromagnetic phase (AF), in which the two phases are antiferromagnetically ordered, when I is negative and predominant in comparison with J'.

(iii) Chiral phases $H_{1,2,3,4}$, in which the two planes have a chiral order, when J is predominant in comparison with I.

We discuss now these chiral phases given in (iii). In the chiral phases, the nonfrustrated plane has almost the ferromagnetic configuration when $I > 0$ or almost the antiferromagnetic configuration when $I < 0$. The Villain plane has almost the 45° configuration when $J > 0$ or the 135° configuration when $J < 0$. Then, there are four possible chiral phases as given below (see Fig.2).

(i) $I > 0$ and $J > 0$ $(J' < 0)$ $(H_1$ phase). In this case, the non-frustrated plane is almost ferromagnetic and the VP has almost the 45° configuration.

(ii) $I > 0$ and $J < 0$ $(J' > 0)$ $(H_2$ phase). In this case, the non-frustrated plane is almost ferromagnetic and the VP has almost the 135° configuration.

(iii) $I < 0$ and $J > 0$ $(J' < 0)$ $(H_3$ phase). In this case, the non-frustrated plane is almost antiferromagnetic and the VP has almost the 45° configuration.

(iv) $I < 0$ and $J < 0 (J' > 0)$ $(H_4$ phase). In this case, the non-frustrated plane is almost antiferromagnetic and the VP has almost the 135° configuration.

In each case, both structures are incomplete and the angle of each spin changes according to the values of the interaction parameters.

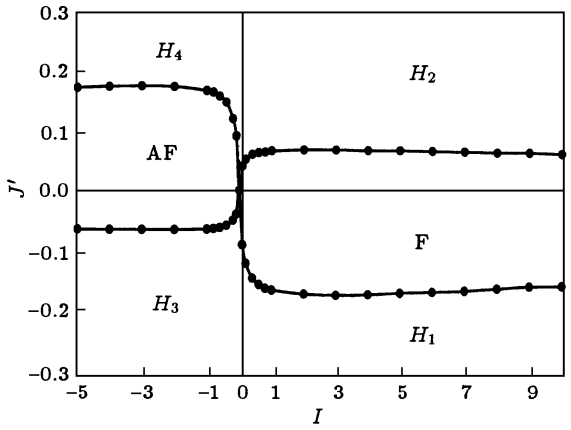


Fig.2. Ground-state phase diagram in (I, J') plane. See text for details of each phase.

3. Results by MC histogram simulation

We use in the present paper the histogram MC technique developed by Ferrenberg and Swendsen.[17] We use the system of $N = 2N_l^2$ spins where $N_l = 24, 32, 40, 52, 80, 92$ and 140, with periodic boundary conditions. We first estimate by the standard MC simulations the critical temperature $T_0(N_l)$ as precise as possible for each N_l and then calculate the energy

histogram $P(E)$ (E is the system energy) at that temperature. For the histogram calculation, we discarded 10^6 or 2×10^6 MC steps per spin for equilibrating the system and calculated the energy histogram as well as other physical quantities over 10^6 or 2×10^6 MC steps. From $P(E)$ at $T_0(N_1)$, we calculate the following quantities at a temperature T close to $T_0(N_1)$:

$$C=\frac{<\mathcal{H}^2>-<\mathcal{H}>^2}{2NT^2}, \tag{2}$$

$$\chi=\frac{<\mathcal{K}^2>-<\mathcal{K}>^2}{T}, \tag{3}$$

$$(\ln<\mathcal{K}>)'=-\left(\frac{<\mathcal{K}\mathcal{H}>}{<\mathcal{K}>}-<\mathcal{H}>\right), \tag{4}$$

where C is the specific heat per site, χ the chiral susceptibility per site; $<\cdots>$ means the thermal average, and the prime denotes the derivative with respect to $\beta=1/(k_{\rm B}T)$. We set the Boltzmann constant $k_{\rm B}$ to 1 in the present paper. The chirality is defined at a smallest up-square, namely an elementary upward square $1,2,3,4$, on each VP or FP as follows:

$$\mathcal{K}^s_{1234}=(-\boldsymbol{s}_1\times\boldsymbol{s}_2+\boldsymbol{s}_2\times\boldsymbol{s}_3+\boldsymbol{s}_3\times\boldsymbol{s}_4+\boldsymbol{s}_4\times\boldsymbol{s}_1)\cdot\hat{e}_z,$$
$$\mathcal{K}^t_{1234}=(\boldsymbol{t}_1\times\boldsymbol{t}_2+\boldsymbol{t}_2\times\boldsymbol{t}_3+\boldsymbol{t}_3\times\boldsymbol{t}_4+\boldsymbol{t}_4\times\boldsymbol{t}_1)\cdot\hat{e}_z. \tag{5}$$

Here $\hat{e}_z$ is the unit vector in the Z-direction in spin space. A set of site 1234 indicates an allocation of sites counterclockwise on each up-square of the lattice VP or FP. The averaged chirality for the whole system is defined by

$$\mathcal{K}=\frac{1}{2}(\mathcal{K}_s+\mathcal{K}_t), \tag{6}$$

where

$$\mathcal{K}_s=\frac{1}{N}\sum_{(1234)}<\mathcal{K}^s_{1234}>,$$
$$\mathcal{K}_t=\frac{1}{N}\sum_{(1234)}<\mathcal{K}^t_{1234}>, \tag{7}$$

where the sum with (1234) is taken over all of the elementary up-square on lattice VP or FP.

Our method for calculating the various quantities and for estimating the error is the following. (i) For a given size N_1, we estimate the critical temperature $T_0(N_1)$ as precisely as possible by standard MC simulations. Let the error of $T_0(N_1)$ be equal to $\pm\Delta$. Then we make histogram measurements at that temperature and calculate various physical quantities using Eqs.(2)–(7). (ii) Next, we make histogram measurements at several temperatures (4 to 8 values of temperature) in a temperature range within the error of $T_0(N_1)$, i.e. from $T_0(N_1)-\Delta$ to $T_0(N_1)+\Delta$. For each obtained histogram, we calculate again various physical quantities. (iii) We average the calculated physical quantities. (iv) We repeat steps (i) to (iii) for other sizes N_1. The above method is known as multihistogram MC technique.

We have determined the nature of the transitions at $J'=-6,-1,1$ and 6. For $J'=-1$ and $J'=1$, the transition at the higher critical temperature is of the KT type. We found that the peak height of the specific heat is independent of N_1 when we plotted the height values $C_{\rm top}$ as a function of N_1, although we have not shown it in the present paper. In the same way the transition that occurs at the lower critical temperature for $J'=6$ and -6 is also of the KT type (see the phase diagram in Fig.10). Now we will present the finite size scaling study for the other transitions.

1) $J'=1$ and -1

We show in Figs.3–6 finite size scaling analysis for -1. Note that the error from the averaging is smaller than the size of the data points shown in the graphs. We find the critical temperature $T_{\rm c}=0.507(4)|J|$ and $T_{\rm c}=0.468(5)|J|$ for $J'=1$ and $J'=-1$, respectively. Using the slope of this graph, we obtain the value of critical exponents as $\nu=0.95(4),\gamma=1.75(3)$ and $\beta=0.15(1)$ for $J'=1$ and $\nu=0.98(3)$, $\gamma=1.78(2)$ and $\beta=0.135(4)$ for $J'=-1$.

These values of critical exponents are also very close to those of the Ising universality class. Then, we think that the transition for $-4<J'<3$, at the lower critical temperature, is of the Ising type.

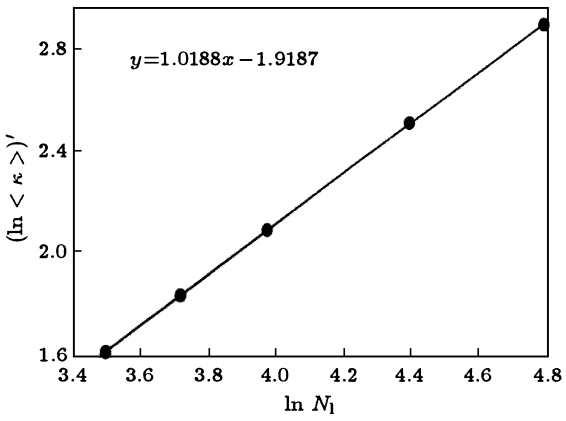


Fig.3. Maximum of $(\ln<\mathcal{K}>)'$ vs $\ln N_1$ for $J'=-1$. The slope of the curve is to $1/\nu=1.0188$ and there is no fitting error.

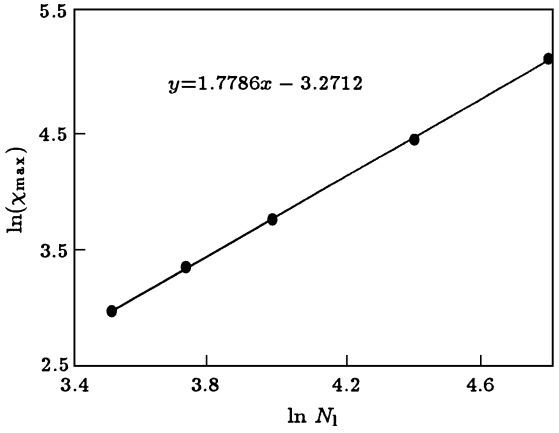


Fig.4. Maximum of the susceptibility χ as a function of N_l in a ln-ln scale for $J' = -1$. The slope yields $\gamma/\nu = 1.7786$ and the fitting error is less than 0.02%.

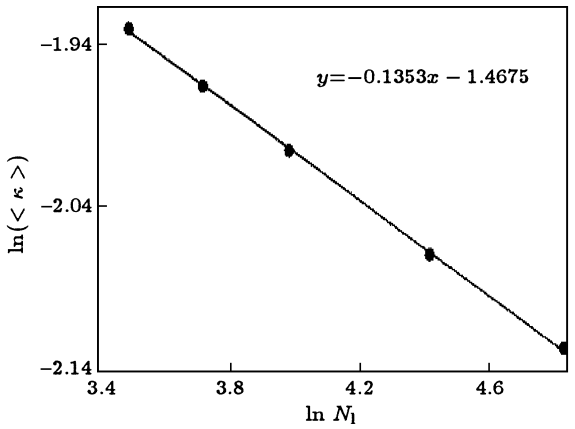


Fig.5. $< \mathcal{K} >$ at $T_c(N_l)$ as a function of N_l in a ln-ln scale for $J' = -1$. The slope yields $\beta/\nu = 0.1353$ and the fitting error is less than 0.04%.

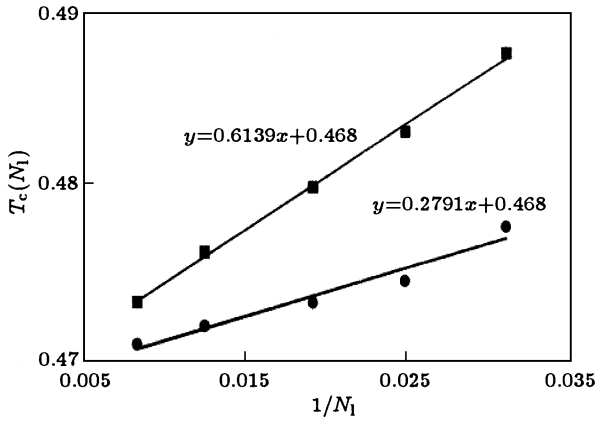


Fig.6. Critical temperature T_c at the maxima of C (circle) and χ (square) for $J' = -1$. We have $T_c(\infty) = 0.4680$ for C and $T_c(\infty) = 0.4680$ for χ and the fitting error is less than 4% and 0.3%, respectively.

2) $J' = 6$ and -6

Now we will see that the transition at $J' = -6$ belongs to the XY Ising universality class. Fig.7 shows the maximum of $(\ln < \mathcal{K} >)'$ versus $\ln N_l$ with $N_l = 24, 32, 40, 52, 80, 92$ and 140. We can see an excellent straight line with a fitting error less than 0.03%. The slope of this curve is equal to $1/\nu$ and then gives $\nu = 0.850(25)$. This value is close to $\nu = 0.85(3)$ obtained by Lee *et al*[11] and $\nu = 0.852(2)$ obtained by Boubcheur and Diep [12] using the coupled XY Ising model, but differs from $\nu = 0.813$ obtained by Lee *et al*[13] and $\nu = 0.889$ obtained by Jeon *et al.*[14]

The value of critical exponent γ is obtained by plotting $\ln \chi_{max}$ versus $\ln N_l$ (Fig.8). We find $\gamma = 1.521(41)$. This value is different from $\gamma = 1.448(24)$ obtained by Lee *et al*[11] but it is close to the $\gamma = 1.531(3)$ obtained by Boubcheur and Diep.[12] The values of critical exponent β is obtained by plotting $\ln < \mathcal{K}(T_c) >$ versus $\ln N_l$. We find $\beta = 0.110(15)$. This value is different from $\beta = 0.08(2)$ obtained by Boubcheur and Diep,[12] but it is very close to $\beta = 0.13(1)$ obtained by Lee *et al.*[11] Note, however, that Boubcheur and Diep [12] obtained beta by using the scaling relation $d\nu = \gamma + 2\beta$. Using this relation we find also $\beta = 0.09(3)$. The hyperscaling relation $\alpha = 2 - d\nu$ gives $\alpha = 0.30(3)$. In order to obtain α, we use the traditional finite-size scaling analysis for the specific heat (see Fig.9). We find $\nu = 0.852$ and $\alpha = 0.377$. These values are consistent with those obtained above. In conclusion, we obtained values of critical exponents at $T_c = 0.4541(5)|J'|$ as $\nu = 0.850(25), \gamma = 1.521(41), \beta = 0.110(3)$ and $\alpha = 0.300(25)$. For $J = 6$, we obtained values of critical exponents at $T_c = 0.4527(6)|J'|$ as $\nu = 0.853(13), \gamma = 1.518(9), \beta = 0.103(13)$ and $\alpha = 0.294(13)$. These results tend to show that the transition at the higher critical temperature for $J' < -4$ and $J' > 3$ belongs to the XY Ising transition.

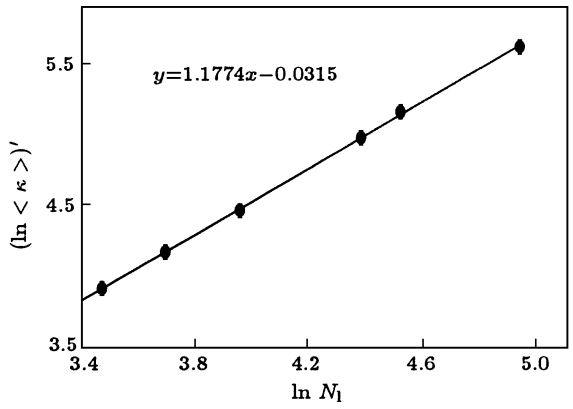


Fig.7. Maximum of $(\ln < \mathcal{K} >)'$ vs $\ln N_l$ for $J' = -6$. The slope of the curve is $1/\nu = 1.1774$ and the fitting error is less than 0.03%.

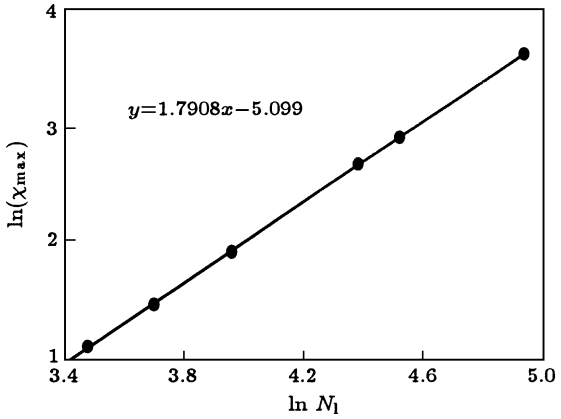


Fig.8. Maximum of the susceptibility χ as a function of $N_{\rm l}$ in a ln-ln scale for $J' = -6$. The slope yields $\gamma/\nu = 1.7908$ and the fitting error is less than 0.01%.

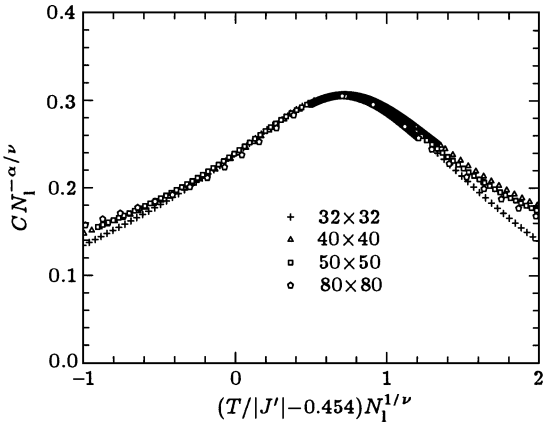


Fig.9. Finite-size analysis for the specific heat given for $J' = -6$. The abscissa is $(T/|J'| - 0.454)N_{\rm l}^{1/\nu}$ with $\nu = 0.852$ and the ordinate is $CN_{\rm l} = N_{\rm l}^{-\alpha/\nu}$ with α=0.377.

In short, we found three kinds of transitions: the KT transition associated with appearance of the quasi-long range order, the Ising transition and XY Ising transition associated with the appearance of the chiral order.

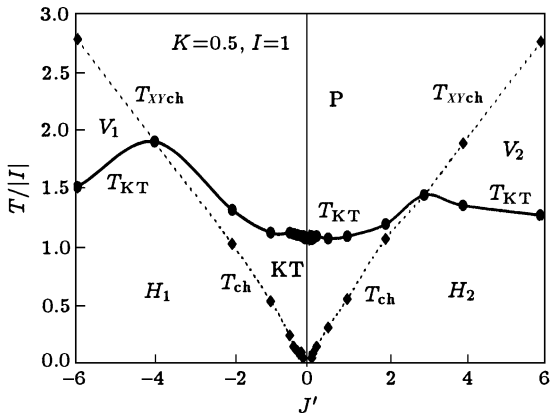


Fig.10. Phase diagram in the space (J', T) for $K = 0.5$ and $I = 1$. See text for details of each phase.

We show in Fig.10 the phase diagram (J', T) for $K = 0.5$ and $I = 1$. This phase diagram presents four phases: (i) A KT phase with a ferromagnetic ground state for $-0.18 < J' < 0.07$. The two planes contain a quasi-long-range order due to the vertex configuration. (ii) Two chiral phases H_1 and H_2. In the H_1 phase, J' is negative ($J > 0$) and hence the configuration of the VP is close to 45° configuration and that of the FP is almost of the KT type with a small value of chirality. In the H_2 phase, J' is positive ($J < 0$), the configuration of the VP is close to 135° configuration and the FP is almost of the KT type with a very small value of chirality. (iii) There are two phases V_1 and V_2 for $J' < -4$ and for $J' > 3$. In these phases the FP is almost paramagnetic with a very small value of chirality but the VP always contains the chiral order. The VP has almost the 45° configuration in the V_1 phase and almost 135° in the V_2 phase. (iv) The paramagnetic phase, P, at higher temperature. In the V_1 and V_2 phase, the FP is almost paramagnetic because there is no $U(1)$ symmetry for temperature greater than the KT transition and chirality in this plane is very small. In fact, we find that the chirality in the FP is very small or almost equal to zero for $J' = -6$ and 6, respectively. Such as $J' = -6$, we have $\mathcal{K}_{\rm F} = 0.005$ at $T = 0$. Then, the inter-layer interaction, $K = 0.5$, is not enough strong, in comparison with $-4 < J' < 3$, to maintain a chiral order in the VP plane. When J' is in the interval $-4 < J' < 3$, the chiral transition in the VP occurs at a lower temperature than the KT transition temperature in the FP. This is due to the fact that the correlations due to the interaction I are stronger than the correlations due to the J' and J interactions. On the other hand, when $J' < -4$ or $J' > 3$, the interactions in the VP are stronger than the interactions in the FP, then the KT transition in the FP occurs at a lower temperature than the transition in the VP. We have shown that there are three kinds of transition: namely, the KT transition due to the appearance of the quasi-long-range order in the FP, the Ising transition due to the appearance of chiral order in the VP when $-4 < J' < 3$ and the XY Ising transition due to the appearance of the chiral order in the VP when $J' < -4$ and $J' > 3$.

4. Concluding remarks

In summary, we have studied the phase transition of an XY model on a two-layer square lattice, which consists of a VP and a FP by an extensive MC histogram technique. According to values of interaction

parameters (I, J'), the system presents three phases: namely, a KT phase in which the two planes are critical for I predominant over J, a chiral phase in which the two planes have a chiral order for J predominant over I, and a new phase, at higher temperature, in which only the VP has a chiral order and the FP is paramagnetic. The results show two kinds of transitions: the usual Ising transition when J' is in the interval $-4 < J' < 3$ and the XY Ising transition outside of this interval. The difference in the behaviours is easily comprehensible. When J' is in the interval $-4 < J' < 3$, the chiral transition in the VP occurs at a lower temperature than the transition in the FP. This is due to the fact that the correlations due to the interaction I are stronger than the correlations due to the J' interactions. But, the presence of the $U(1)$ symmetry in the FP tends to maintain the $U(1)$ symmetry also in the VP. In consequence, the chiral transition is due to the disappearance of all the Z_2 symmetry and some part of the $U(1)$ symmetry of the VP. This gives the Ising-type transition.

In the opposite way, when $J' < -4$ or $J' > 3$, the interaction constants in the VP are stronger than the interaction constant in the FP, then the KT transition in the FP occurs at a lower temperature than the transition in the VP. The transition in the FP does not affect the symmetry of the VP that keeps the $U(1)$ and Z_2 symmetry. In consequence, the chiral transition that occurs at a higher temperature than the KT transition is associated with the disappearance of both the Z_2 symmetry (Ising) and $U(1)$ symmetry (KT) of the VP.

In conclusion, this work confirms the existence of two kinds of transitions in the canted XY Ising spin model, namely the Ising transition when the system contains a strong Z_2 symmetry and the XY Ising transition when the system contains both the Z_2 symmetry and the $U(1)$ symmetry.

References

[1] Anderson F B and Callen H B 1964 *Phys. Rev.* A **136** 1068

[2] Mills D L and Saslow W M 1968 *Phys. Rev.* **171** 488

[3] Mills D L 1968 *Phys. Rev. Lett.* **31** 18

[4] Keffer F and Chow H 1973 *Phys. Rev. Lett.* **31** 1061

[5] Trallori L, Politi P, Rettori A, Pini M G and Villain J 1994 *Phys. Rev. Lett.* **72** 1925

[6] Maccio M, Pini M G, Trallori L, Politi P and Rettori A 1995 *Phys. Lett.* A **205** 329

[7] Momma M and Horiguchi T 1998 *Physica* A **259** 105

[8] Horiguchi T, Wang Y and Honda Y 1998 *Physica* A **260** 131

[9] Berge B, Diep H T, Ghazali A and Lallemand P 1986 *Phys. Rev.* B **34** 3177

[10] Nightingale M P, Granato E and Kosterlitz J M 1995 *Phys. Rev.* B **52** 7402

[11] Lee J, Kosterlitz J M and Granato E 1991 *Phys. Rev.* B **43** 11531
Granato E, Kosterlitz J M, Lee J and Nightingale M P 1991 *Phys. Rev. Lett.* **66** 1090

[12] Boubecheur E H and Diep H T 1998 *Phys. Rev.* B **58** 5163

[13] Lee S and Lee K C 1994 *Phys. Rev.* B **49** 15184

[14] Jeon G S, Park S Y and Choi M Y 1997 *Phys. Rev.* B **55** 14088

[15] Ramirez-Santiago G and Jose J V 1994 *Phys. Rev.* B **49** 9567

[16] Olsson P 1995 *Phys. Rev. Lett.* **75** 2758

[17] Ferrenberg A M and Swendsen R H 1988 *Phys. Rev. Lett.* **61** 2635
Ferrenberg A M and Swendsen R H 1989 *Phys. Rev. Lett.* **63** 1195